Indonesian Physical Review
Volume 09 Issue 03, September 2026
P-ISSN: 2615-1278, E-ISSN: 2614-7904

Experimental Investigation on Electrical Load Characteristics of a Monocrystalline Photovoltaic Panel under RGB-Filtered Broadband LED Illumination

M. Raynaldo Sandita Powa[1,2*], Afrizal Mayub[1], Euis Nursaadah[1*]
[1] *Graduate School of Science Education, University of Bengkulu, Bengkulu, 38371, Indonesia*
[2] *State Vocational High School no. 2 Empat Lawang, Empat Lawang, Indonesia, 31593, Indonesia*

Corresponding Authors E-mail: euis@unib.ac.id, raynaldo.sandita@gmail.com

Article Info

Article info:
Received: 18-02-2026
Revised: 26-06-2026
Accepted: 06-07-2026

Keywords:
Filtered broadband illumination; Indoor PV testing; Electrical load characteristics; RGB filtering; Photometric illuminance

How To Cite:
M. R. S. Powa, A. Mayub, E. Nursaadah, "Experimental Investigation on Electrical Load Characteristics of a Monocrystalline Photovoltaic Panel under RGB-Filtered Broadband LED Illumination", Indonesian Physical Review, vol. 9, no. 3, p 439-451, 2026.

DOI:
https://doi.org/10.29303/ipr.v9i3.659.

Abstract

RGB-filtered broadband illumination was applied to a monocrystalline photovoltaic (PV) panel under controlled indoor conditions to observe its electrical load characteristics. Optical red, green, and blue filters are used to produce RGB channel dominance in the transmitted light from a 5000 K LED source, without implying narrowband spectral separation. Sequential resistive loads (10 steps from 100 Ω to 4700 Ω) are applied to generate voltage–current operating points that reconstruct I–V and P–V characteristics under each filtering condition. Standard PV parameters, including estimated short-circuit current (I_{sc}), open-circuit voltage (V_{oc}), maximum power point (MPP), and estimated fill factor (FF), are derived from load-based curve extrapolation. Lux measurements are recorded alongside the electrical data to provide a comparison with photometric brightness. The results show a consistent ordering of electrical performance: green-filtered illumination produces higher current and power output than red or blue illumination under the present experimental conditions. The maximum power under green filtering is approximately 54% higher than under red filtering and more than 400% higher than under blue filtering. However, since irradiance and spectral power distribution are not measured, differences in transmitted light intensity across filters may also contribute to the observed electrical variations, along with wavelength-related effects. The comparison using Isc/Lux and Pmax/Lux is presented only as an illustrative indicator and does not represent a physically rigorous photovoltaic performance metric. Therefore, the findings are interpreted as RGB-filtered broadband effects that are qualitatively consistent with known silicon spectral response behavior, rather than as direct spectral characterization. This work provides a practical, low-cost indoor protocol to observe photovoltaic response trends using accessible instrumentation without spectroradiometric equipment.

Introduction

Crystalline silicon photovoltaic (PV) panels are not governed solely by the apparent brightness of incident light. How that light is distributed across wavelengths also plays a role, since photon energy determines the generation of charge carriers in silicon, as determined by its spectral response [1][2]. Consequently, two light sources with similar photometric brightness (lux) can produce different electrical outputs, because photovoltaic performance is governed by radiometric quantities, such as irradiance (W/m^2) and photon flux, and depends on the spectral distribution of the incident light [1][3]. As a result, photometric brightness alone is insufficient to describe the energy relevant to photovoltaic conversion, particularly when the spectral composition of the light source varies.

Spectral variations under both natural sunlight and artificial lighting have been reported to influence PV performance in measurable ways. Outdoor spectral measurements and spectral mismatch analyses, for example, show that PV electrical behavior follows spectral irradiance rather than perceived brightness [4][5][6]. However, most of these approaches rely on spectroradiometric instrumentation, numerical modeling, or standardized spectra, which are not easily accessible for simple laboratory-scale experimentation [7][8]. Accurate isolation of wavelength-dependent effects typically requires controlled radiometric measurements or narrowband illumination, which are not accessible in many low-cost experimental environments.

A practical challenge is how to explore observable spectral-related effects using a simple indoor setup without spectroradiometric equipment. Long-term spectral monitoring systems such as those reported by Conde et al. [9] provide detailed data, but they are not intended for short-term, low-cost laboratory experimentation. In this study, optical red, green, and blue (RGB) filters are placed in front of a 5000 K LED source to modify the spectral composition of the broadband light transmitted to the PV panel. Similar LED–PV interactions have been discussed by Qaid et al. [10], and polychromatic filtering approaches have previously been applied in photovoltaic studies without monochromatic sources [11][12][13].

A synchronized Arduino-based measurement system is employed to record voltage, RGB channel intensity, and illuminance in real time under controlled indoor conditions. Photometric lux measurements are included as a pedagogical contrast to demonstrate that perceived brightness is not proportional to photovoltaic output. PV performance should ideally be compared to irradiance (W/m^2) or photon flux, which are not measured in this setup and are therefore acknowledged as a limitation [14][15].

In this context, the research gap addressed in this study is the limited availability of simple, low-cost experimental approaches for observing wavelength-related trends in photovoltaic response, as most existing studies rely on spectroradiometric measurements or controlled spectral sources. To address this gap, this work focuses on three practical aspects: (i) proposing a filter-based indoor protocol to modify light composition in a controlled manner, (ii) reconstructing I–V and P–V characteristics using sequential resistive loads, and (iii) demonstrating quantitative trends illustrating that photometric illuminance is not proportional to PV electrical response. The results are interpreted as observable trends consistent with silicon spectral response behavior rather than as direct spectral characterization [16][17].

Experimental Method

Instrumentation Setup

A low-cost integrated instrumentation system based on an Arduino Nano was developed to synchronously record electrical, photometric, and colorimetric data from a small monocrystalline photovoltaic (PV) panel in real time. The PV panel used in this study has dimensions of 135 mm × 125 mm, with a nominal operating voltage of 5 V, a maximum open-circuit voltage (Voc) of 6 V, and a maximum short-circuit current (Isc) of 400 mA (with a typical operating current of approximately 360 mA). These specifications provide a reference for the panel's operating range under the experimental conditions.

Voltage was measured using an INA219 sensor configured only for bus-voltage reading. Current was not taken directly from the sensor but calculated from the measured voltage and the applied resistive load using Ohm's law. This approach avoids the burden voltage of the INA219 shunt and keeps the load-defined operating point of the panel.

The resistive loads used in this study ranged from 100 Ω to 4700 Ω (10 discrete steps). All resistors had a manufacturer's tolerance of ±1%, and wiring/contact resistance was assumed negligible compared to the load magnitude. This tolerance introduces a bounded uncertainty in the calculated current values, which is consistent across all RGB filtering conditions.

Photometric illuminance was measured with a BH1750 lux sensor, and RGB channel intensities were monitored with a TCS34725 sensor. TCS34725 measures only relative RGB channel dominance in the received light. The BH1750 digital lux sensor was used to monitor photometric illuminance as an indicator of lighting stability and relative illumination differences among the RGB filtering conditions. Although illuminance (lux) is not equivalent to radiometric irradiance (W/m²), it provides a practical photometric reference for evaluating relative changes in lighting conditions when spectroradiometric measurements are unavailable. A synchronized Arduino-based acquisition system allows real-time monitoring of optical and electrical parameters under controlled indoor conditions. Similar low-cost optical sensor approaches integrated with microcontroller-based data acquisition have been demonstrated for quantitative optical measurements by Syafutra et al. [18], supporting the validity of such instrumentation for experimental optical studies without requiring complex spectroradiometric equipment.

The sensors (INA219 and BH1750) were validated against reference instruments, including a digital multimeter and a commercial lux meter (Kuber AS803). Validation was conducted under controlled indoor illumination using a 5000 K COB LED source. Multiple measurements across varying operating conditions showed strong linear agreement ($R^2 \approx 0.9999$) with bounded measurement errors. The INA219 sensor exhibited an absolute current error of approximately 2 mA (≈6.7%), while voltage measurements showed errors below 1%. The BH1750 sensor demonstrated relative errors below 3%. These results indicate that the sensors provide sufficiently consistent measurements for comparative experimental analysis, although no formal calibration traceable to radiometric standards was performed.

A Krisbow 5000K COB LED (rated power 10 W, illumination output 100 LM/W) served as the illumination source. The optical arrangement was placed inside a matte-black enclosure (54,5 cm × 39 cm × 49 cm) to minimize reflections and external light interference. The LED, RGB filter, PV panel, and sensors were fixed at constant positions throughout all experiments to maintain consistent illumination geometry. Keeping the illumination geometry within the

enclosure reduces irradiance nonuniformity and geometric effects, which are known to influence indoor PV electrical response independently of spectral composition [19]. Although irradiance (W/m²) and spectral power distribution were not measured, the fixed geometry ensured that comparisons were made under repeatable indoor conditions.

Commercial RGB filters (color gel filter card) commonly used in photography lighting were employed to modify the broadband light transmitted by the 5000 K white LED before it reached the photovoltaic panel. The spectral transmittance characteristics of these filters were not formally measured. Therefore, their effect is interpreted in terms of RGB channel dominance rather than precise spectral control.

A block diagram of the experimental setup, including the optical path, electrical loading path, and data acquisition system, is shown in Figure 1. An experimental setup, including the electrical connections between the photovoltaic panel, the resistive load, the INA219 sensor, and the Arduino-based data acquisition system, is shown in Figure 2.

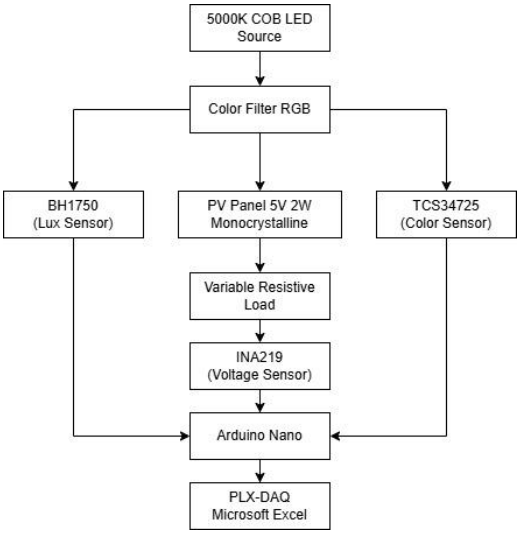

Figure 1. Block diagram of the integrated measurement system illustrating the optical path, electrical loading path, and synchronized data acquisition using Arduino-based sensors.

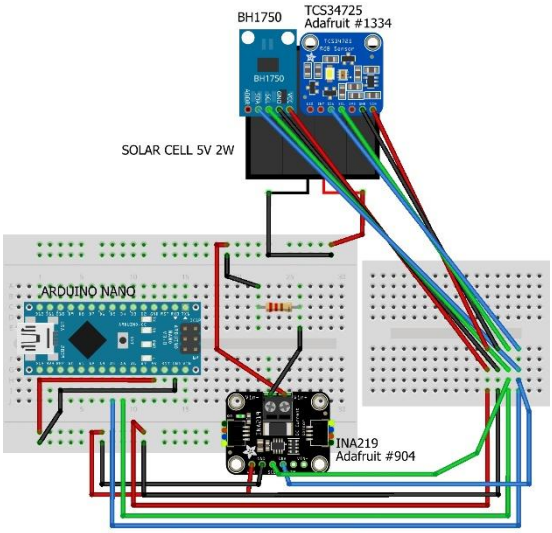

Figure 2. Experimental setup showing the electrical connections between the photovoltaic panel, the resistive load, the INA219 sensor, and the Arduino-based data acquisition system.

A similar polychromatic filtering approach has been previously used to investigate photovoltaic response trends without the need for monochromatic light sources [11][12][13]. In this study, optical red, green, and blue filters were positioned between the LED source and the PV panel to produce RGB channel dominance in the transmitted broadband light. The LED was placed 8 cm from the filter, and the filter was positioned 54 cm from the panel. This geometry was kept constant across all experiments to ensure that differences in electrical output were due to changes in color composition rather than to variations in distance or illumination distribution.

The TCS34725 sensor was used prior to data acquisition to confirm that each filter produced a clear dominance of the intended RGB channel. Only after the RGB readings reached stable dominance were electrical measurements conducted. This confirms that the observed

electrical variations are associated with RGB channel dominance rather than geometric or temporal effects.

Measurement Procedure

The electrical behavior of the PV panel was characterized by applying a sequence of resistive loads: 100 Ω, 150 Ω, 220 Ω, 330 Ω, 470 Ω, 680 Ω, 1000 Ω, 2000 Ω, 3300 Ω, and 4700 Ω. Each resistor produces a distinct electrical operating point represented by a voltage–current pair. Voltage was measured directly, while current was calculated using Ohm's law:

$$I = \frac{V}{R}$$

where I is the current (A), V is the voltage (V), and R is the resistance (Ω).
These measurements produce a set of operating points across different load conditions, which collectively form electrical characteristics resembling I–V and P–V curves of the PV panel under each RGB illumination condition [20].

True short-circuit ($R \approx 0\ \Omega$) and open-circuit ($R \to \infty$) conditions were not applied. Therefore, short-circuit current (Isc) and open-circuit voltage (Voc) were estimated by linearly extrapolating the operating points near the respective curve ends. Maximum power point (Vmp, Imp) and the estimated fill factor (FF) were derived from the reconstructed curves, following the parameter-extraction principles described by Humada [21]. Because the I–V curve is reconstructed from a limited number of discrete load points, particularly with sparse sampling near the knee region, the extracted fill factor (FF) values are treated as approximations rather than exact representations of diode characteristics. This interpretation is consistent with prior studies indicating that photovoltaic parameters derived from I–V measurements are subject to estimation uncertainty, approximation, and measurement-related errors [22][23].

The COB LED exhibits thermal stabilization after power-on, resulting in a gradual change in lux. To avoid this effect, only data within the plateau region of lux stabilization were selected. For each load, 10–15 consecutive samples within this stable interval were averaged to represent steady-state conditions. Data were recorded at approximately 60-second intervals.

RGB channel dominance was verified before each measurement using the TCS34725. This verification confirms color channel dominance, not spectral characterization. RGB dominance verified by the TCS34725 should therefore be interpreted only as filtered broadband channel dominance rather than as control of the actual spectral power distribution at the PV surface [19]. Photometric lux measurements are included as a pedagogical comparison. As discussed by Tabaka [14] and by Hamadani [15], PV performance should ideally be compared to irradiance or photon flux, which are acknowledged as limitations in this setup.

Control of Confounding Factors

Several factors were controlled during the experiment to maintain consistent illumination conditions. The geometry between the LED source, optical filter, and PV panel was kept fixed throughout all experiments, and the entire optical arrangement was placed inside a matte-black enclosure to suppress internal reflections and external light interference. Measurements were conducted in a stable indoor environment to minimize temperature variation, and the same set of resistive loads was used consistently across all RGB conditions. The same data acquisition procedure was used for all filtering conditions. RGB filters modify both the color composition and the total transmitted light intensity. Because irradiance was not measured,

part of the electrical variation may also be affected by differences in total transmitted light power.

Result and Discussion

Verification of RGB Channel Dominance using RGB Sensor

RGB measurements were first used to confirm the channel dominance of each optical filter at the panel surface. Continuous RGB monitoring using the TCS34725 sensor shows that under the red filter, the R component is consistently much higher than G and B. Similar dominance patterns are observed for the green and blue filters, where the respective color component remains dominant throughout the measurement period. This dominance remained stable during the same interval used for electrical data acquisition. The stabilization of lux values confirms that steady illumination conditions were achieved before data acquisition, as shown at Figure 3.

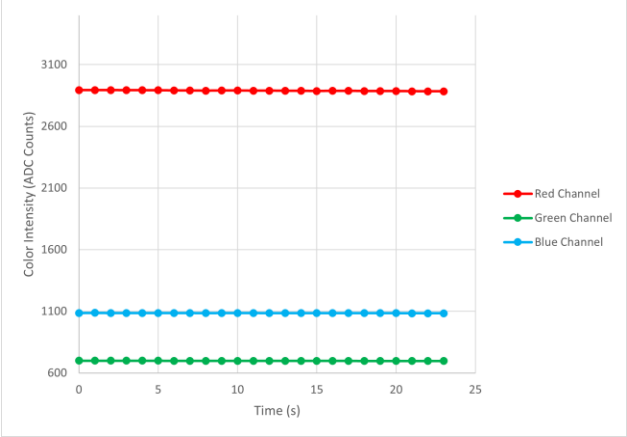

Figure 3. RGB Intensity Stabilization Over Time under Red Filter Illumination (R=1000Ω)

Electrical Load Characteristics Resembling *I–V* and *P–V* Behavior

By applying sequential resistive loads, each RGB illumination condition produced a set of voltage–current operating points. When arranged by voltage, these points form patterns resembling *I–V* characteristics. Plotting power versus voltage produces curves resembling P–V behavior, as shown in Figures 4 and 5.

Across the entire load range, green-dominated illumination consistently produces current values approximately 44% higher than red and approximately 5.8 times higher than blue under the present conditions. This ordering follows trends reported in studies of spectral effects on photovoltaic performance [24][6].

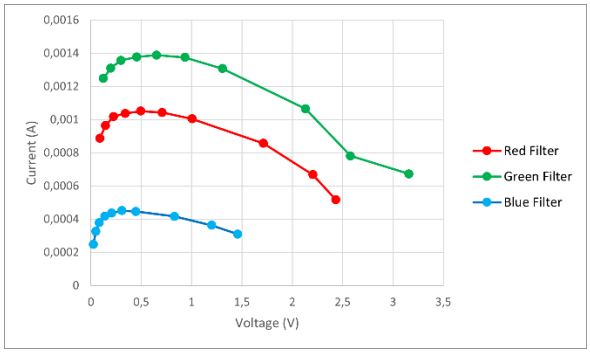

Figure 4. Electrical Load Characteristics Resembling *I–V* Curves of the PV Panel Under RGB Illumination

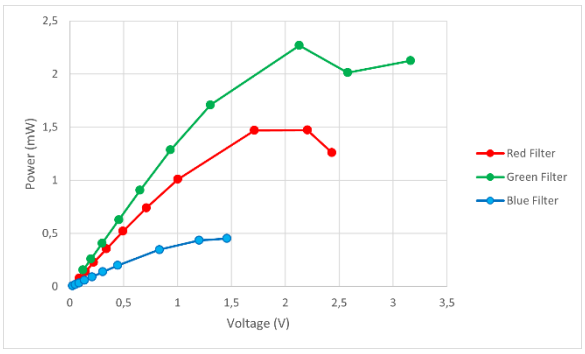

Figure 5. Electrical Load Characteristics Resembling *P–V* Curves of the PV Panel Under RGB Illumination

A similar ordering is observed in the P–V curves, where the maximum power under green filtering is noticeably higher than under red or blue illumination. The maximum power (P_{max}) under green filtering is approximately 54% greater than under red and about 400% greater than under blue, providing a quantitative comparison between conditions. The measurements in this study were conducted using a single acquisition sequence for each load condition under stabilized illumination. To reduce short-term fluctuations, each reported data point represents the average of 10–15 consecutive samples within the steady-state region. While this approach improves temporal stability, it does not capture variability across repeated trials. Therefore, no statistical dispersion metrics such as standard deviation or error bars are reported. This limitation should be considered when interpreting the results, as the absence of repeated measurements restricts the ability to quantify experimental uncertainty.

This behavior follows the known wavelength-dependent response of crystalline silicon, in which the absorption depth and recombination probability vary with photon wavelength within the semiconductor, as described by Würfel [16] and Nelson [17]. Short-wavelength photons (blue region) are absorbed very close to the front surface, increasing the probability of front-surface recombination. Long-wavelength photons (red region) penetrate deeper, where reduced absorption increases the likelihood of recombination near the rear of the cell. Mid-visible wavelengths (green region) offer a better balance between absorption depth and carrier collection efficiency. The ordering observed in this experiment is consistent with this well-established silicon behavior under RGB-filtered broadband illumination.

Estimation of Standard PV Parameters from Load-Derived Characteristics

From the reconstructed electrical characteristics, standard PV parameters, including estimated short-circuit current (Isc), estimated open-circuit voltage (Voc), maximum power voltage (Vmp), maximum power current (Imp), and estimated fill factor, were extracted from the reconstructed characteristics using linear extrapolation and curve-based estimation following Humada [21].

Table 1. Estimated electrical parameters under RGB illumination.

Color Filter	Estimated Electrical Parameters				
	Est I_{sc} (A)	Est V_{oc} (V)	Est V_{mp} (V)	Est I_{mp} (A)	Est *FF*
Red	8.13×10^{-4}	3.598	2.204	6.68×10^{-4}	0.503
Green	11.74×10^{-4}	4.876	2.130	10.65×10^{-4}	0.396
Blue	2.02×10^{-4}	3.355	1.458	3.10×10^{-4}	0.667

The largest variation appears in I_{sc}, following the same ordering as current and power. In contrast, V_{oc} values show relatively smaller variations between filtering conditions, ranging from approximately 3.36 V to 4.88 V across RGB illumination. The higher V_{oc} observed under blue filtering, despite its low I_{sc}, is consistent with the logarithmic dependence of V_{oc} on photocurrent generation. V_{oc} is estimated from discrete operating points near the open-circuit region and is sensitive to extrapolation. This sensitivity is particularly pronounced when the available data points are sparse near the open-circuit condition, increasing the uncertainty of linear extrapolation and potentially leading to overestimation at low current levels, such as under blue-filter illumination.

Differences in estimated fill factor are influenced by the discrete load steps. Since the load steps are discrete and not densely distributed around the curve knee, *FF* variations may partly reflect sampling density rather than intrinsic diode behavior, as discussed by Olayiwola et al. [25] in their parameter extraction from discrete I–V points.

Photometric Illuminance Versus Photovoltaic Output

A comparison between steady-state lux values and electrical parameters shows a nonproportional relationship between photometric brightness and photovoltaic output [26]. As summarized in Table 2 below, green filtering produces approximately twice the lux value of red filtering, yet the corresponding increase in current and maximum power is not proportional.

Table 2. Comparison between lux, I_{sc}, and P_{max} under RGB illumination

Color Filter	Lux (Steady State Average)	Est I_{sc} (A)	Est P_{max} (W)	I_{sc}/Lux	P_{max}/Lux
Red	505.26	8.13×10^{-4}	1.472×10^{-3}	1.61×10^{-6}	2.91×10^{-6}
Green	1070.33	11.74×10^{-4}	2.269×10^{-3}	1.09×10^{-6}	2.12×10^{-6}
Blue	208.3	2.02×10^{-4}	0.452×10^{-3}	0.97×10^{-6}	2.17×10^{-6}

The electrical parameters reported in Table 2 are directly derived from the values in Table 1, specifically the estimated Isc and calculated Pmax. Therefore, there is no independent measurement discrepancy between the two tables. Table 2 reorganizes selected parameters from Table 1, combined with lux measurements, to facilitate comparative analysis. Any apparent differences arise from the inclusion of derived ratios (I_{sc}/Lux and P_{max}/Lux) rather than inconsistencies in the primary electrical data.

This relationship is shown in Figures 6 and 7, where the distributions of Pmax and Isc as a function of lux do not show a linear trend across RGB conditions. Higher perceived brightness does not correspond directly to higher electrical generation. While Figures 6 and 7 are derived from the values summarized in Table 2, they present different relationships (I_{sc}–Lux and P_{max}–Lux), which allow clearer visualization of the non-linear relationship between photometric illuminance and photovoltaic output.

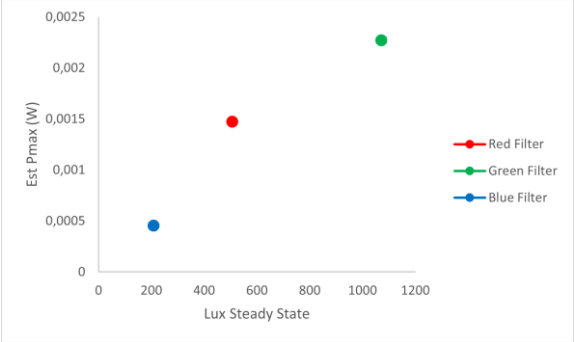

Figure 6. Relationship between photometric illuminance (lux) and maximum power output (P_{max}) under RGB illumination.

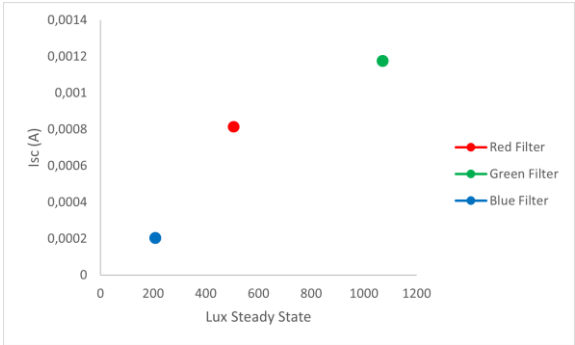

Figure 7. Relationship between photometric illuminance (lux) and short-circuit current (I_{sc}) under RGB illumination.

This comparison illustrates that lux, which follows the photopic response of the human eye as described by Tabaka [14], is not proportional to the radiative energy relevant for semiconductor absorption. Ideally, photovoltaic performance should be compared to irradiance or photon flux, as discussed by Hamadani [15], which were not measured in this study. The ratios I_{sc}/Lux and P_{max}/Lux in Table 2 are presented only as illustrative comparisons.

Interpretation Consistent with Silicon Spectral Response

The light source employed in this study was a white LED with a Correlated Color Temperature (CCT) of 5000 K. Modern white LEDs are generally based on phosphor-converted white LED (pc-LED) technology, in which a blue LED chip excites a phosphor layer that converts part of the blue emission into broadband visible emission, producing white light [27]. This configuration produces a non-uniform spectral power distribution (SPD) rather than equal emission across the visible spectrum, with a narrow blue emission peak and a broad phosphor emission band. The formation of this SPD has been described by Schneider et al. as the superposition of the blue LED emission and the phosphor emission, which together define the characteristic spectral profile of a phosphor-converted white LED [28].

Within the present experimental configuration, the optical conditions incident on the photovoltaic panel were determined by the interaction between the spectral distribution of the white LED source and the spectral transmittance characteristics of the RGB filters employed. Consequently, each filter condition represents a distinct illumination environment, while all other experimental parameters are held constant. Shen et al. demonstrated that the transmitted spectrum after optical filtering is governed by the

interaction between the emission spectrum of the light source and the spectral transmittance function of the filter, whereas Spitschan et al. emphasized that spectral transmittance is the fundamental optical property determining the amount of light transmitted at each wavelength [29][30]. Accordingly, the findings of the present study are interpreted as the behavior of the photovoltaic system under illumination conditions established by commercial RGB gel filters, rather than as a direct characterization of the intrinsic spectral response of monocrystalline silicon.

The wavelength-dependent spectral response of crystalline silicon explains how absorption depth and carrier recombination probability vary with photon wavelength inside the semiconductor, as described in the photovoltaic physics literature by Würfel [16] and Nelson [17]. Detailed experimental studies on differential spectral responsivity demonstrate that accurate characterization of silicon spectral response requires quasi-monochromatic illumination, controlled bias irradiance, and radiometric calibration across wavelengths, as presented by Kärhä et al. [31].

This experiment uses RGB optical filtering under broadband LED illumination without radiometric measurement. The ordering observed in this study is discussed as trends consistent with the known silicon spectral response behavior under RGB-filtered broadband conditions, rather than as direct spectral characterization.

A key limitation of this experiment is the presence of a spectral–intensity confound. The RGB optical filters simultaneously modify both the spectral composition of the incident light and the total transmitted optical power reaching the photovoltaic surface. As a result, the observed differences in electrical output cannot be attributed solely to spectral effects. Without independent measurement or control of irradiance, spectral power distribution (SPD), or an equivalent radiometric proxy, the interpretation of RGB-dependent trends should be treated cautiously. Therefore, the results presented in this study are interpreted as indicative trends under filtered broadband illumination rather than as a direct characterization of intrinsic spectral response. The primary objective of this study is to demonstrate observable trends under controlled low-cost experimental conditions rather than to establish statistically rigorous photovoltaic characterization.

Conclusion

RGB-filtered broadband illumination produces distinct electrical load characteristics in a monocrystalline photovoltaic panel under controlled indoor conditions. Load-derived operating points form patterns resembling $I–V$ and $P–V$ behavior, enabling the estimation of PV parameters using sequential resistive loads.

Across all loading conditions, green-filtered illumination consistently yields the highest current and maximum power, followed by red, while blue produces the lowest electrical output. This ordering follows the known wavelength-dependent response of crystalline silicon to broadband light filtered through RGB filters and is not intended for direct spectral characterization.

The observed non-proportional relationship between photometric illuminance and photovoltaic output is consistent with established photovoltaic principles, as lux represents a photometric quantity rather than the radiometric input governing semiconductor photo-

generation. Therefore, this behavior is interpreted as an expected outcome under spectrally modified illumination rather than as a novel finding.

This work demonstrates a low-cost indoor experimental protocol for observing comparative photovoltaic response trends associated with RGB channel dominance without requiring spectroradiometric instrumentation, within the scope of exploratory experimental analysis. The findings should be interpreted within the scope of the present experimental conditions. Although radiometric quantities (irradiance and spectral power distribution) were not measured, the proposed methodology provides a practical, low-cost approach for observing comparative photovoltaic behavior under RGB-filtered broadband illumination.

Future work should incorporate radiometric characterization, direct measurement of short-circuit current (Isc) and open-circuit voltage (Voc), repeated trials for uncertainty analysis, and improved load resolution near the maximum power point to enhance experimental rigor.

References

[1] R. Eke, T. R. Betts, and R. Gottschalg, "Spectral irradiance effects on the outdoor performance of photovoltaic modules," *Renewable and Sustainable Energy Reviews*, vol. 69, pp. 429–434, 2017, doi: 10.1016/j.rser.2016.10.062.

[2] G. Lopez *et al.*, "Increasing the Resolution and Spectral Range of Measured Direct Irradiance Spectra for PV Applications," *Remote Sensing*, vol. 15, no. 1675, 2023, doi: 10.3390/rs15061675.

[3] A. Chakraborty *et al.*, "Photovoltaics for indoor energy harvesting," *Nano Energy*, vol. 128, no. PB, p. 109932, 2024, doi: 10.1016/j.nanoen.2024.109932.

[4] D. Leitão, J. P. N. Torres, and J. F. P. Fernandes, "Spectral irradiance influence on solar cells efficiency," *Energies*, vol. 13, no. 19, 2020, doi: 10.3390/en13195017.

[5] G. S. Kinsey *et al.*, "Impact of measured spectrum variation on solar photovoltaic efficiencies worldwide," *Renewable Energy*, vol. 196, pp. 995–1016, 2022, doi: 10.1016/j.renene.2022.07.011.

[6] D. Kouklaki, S. Kazadzis, I.-P. Raptis, K. Papachristopoulou, I. Fountoulakis, and K. Eleftheratos, "Photovoltaic Spectral Responsivity and Efficiency under Different Aerosol Conditions," *Energies*, vol. 16, no. 6644, 2023, doi: 10.3390/en16186644.

[7] M. Tsuji, J. Chantana, K. Nakayama, and Y. Kawano, "Utilization of spectral mismatch correction factor for estimation of precise outdoor performance under different average photon energies," *Renewable Energy*, vol. 157, pp. 173–181, 2020, doi: 10.1016/j.renene.2020.05.017.

[8] I. Bevanda, P. Marić, A. Kristić, and T. Betti, "Assessing the Impact of Solar Spectral Variability on the Performance of Photovoltaic Technologies Across European Climates," *Energies*, vol. 18, no. 14, pp. 1–24, 2025, doi: 10.3390/en18143868.

[9] L. A. Conde, J. R. Angulo, M. Sevillano-Bendezú, G. Nofuentes, J. A. Töfflinger, and J. de la Casa, "Spectral effects on the energy yield of various photovoltaic technologies in Lima (Peru)," *Energy*, vol. 223, 2021, doi: 10.1016/j.energy.2021.120034.

[10] S. M. H. Qaid *et al.*, "Optoelectronic Device Modeling and Simulation of Selenium-Based Solar Cells under LED Illumination," *Crystals*, vol. 13, no. 12, 2023, doi: 10.3390/cryst13121668.

[11] E. C. Gouvêa, P. M. Sobrinho, and T. M. Souza, "Spectral response of polycrystalline silicon photovoltaic cells under real-use conditions," *Energies*, vol. 10, no. 8, pp. 1–13, 2017, doi: 10.3390/en10081178.

[12] I. D. Sara, T. R. Betts, and R. Gottschalg, "Determining Spectral Response of a Photovoltaic Device using Polychromatic Filters," *IET Renewable Power Generation*, vol. 8, no. 8, p. 947, 2014, doi: 10.1049/iet-rpg.2014.0323.

[13] M. Abdelnafea, S. Abulanwar, S. Kaddah, A. Hussain, and M. Tawfik, "Experimental study of photovoltaic performance with a spectral filtration technique," *Results in Engineering*, vol. 24, no. September, pp. 4–10, 2024, doi: 10.1016/j.rineng.2024.103555.

[14] P. Tabaka and J. Wtorkiewicz, "Analysis of the Spectral Sensitivity of Luxmeters and Light Sensors of Smartphones in Terms of Their Influence on the Results of Illuminance Measurements—Example Cases," *Energies*, vol. 15, no. 16, 2022, doi: 10.3390/en15165847.

[15] B. H. Hamadani and M. B. Campanelli, "Photovoltaic Characterization under Artificial Low Irradiance Conditions Using Reference Solar Cells," *IEEE Journal of Photovoltaics*, vol. 10, no. 4, pp. 1119–1125, 2020, doi: 10.1109/JPHOTOV.2020.2996241.

[16] P. Würfel and U. Würfel, "Physics of Solar Cells," in *Wiley-VCH*, vol. 112, 2005, pp. 11–21. doi: 10.1007/3-540-26628-3_2.

[17] J. Nelson, *The Physics of Solar Cells*. London: Imperial College Press, 2003.

[18] H. Syafutra, S. Claudia, E. Rustami, S. D. Hardiningtyas, Supriyanto, and M. Zuhri, "Development of Low-Cost Optical Sensor-Based Device for Real-Time Microalgae Concentration Measurement," *Indonesian Physical Review Volume*, vol. 08, no. 02, 2025, doi: 10.29303/ipr. v8i2.473.

[19] C. Sun *et al.*, "LED-based solar simulator for terrestrial solar spectra and orientations," *Solar Energy*, vol. 233, no. January, pp. 96–110, 2022, doi: 10.1016/j.solener.2022.01.001.

[20] K. Maham, P. Karha, and E. Ikonen, "Spectral Mismatch Uncertainty Estimation in Solar Cell Calibration Using Monte Carlo Simulation," *IEEE Journal of Photovoltaics*, vol. 13, no. 6, pp. 899–904, 2023, doi: 10.1109/JPHOTOV.2023.3311890.

[21] A. M. Humada, M. Hojabri, S. Mekhilef, and H. M. Hamada, "Solar cell parameters extraction based on single and double-diode models: A review," *Renewable and Sustainable Energy Reviews*, vol. 56, pp. 494–509, 2016, doi: 10.1016/j.rser.2015.11.051.

[22] M. Louzazni and S. Al-Dahidi, "Approximation of photovoltaic characteristics curves using Bezier Curve," *Renewable Energy*, vol. 174, pp. 715–732, 2021, doi: 10.1016/j.renene.2021.04.103.

[23] K. Emery, "PV reliability determination from I-V measurement and analysis," in *Reliability of Photovoltaic Cells, Modules, Components, and Systems*, SPIE, 2008. doi: 10.1117/12.795965.

[24] B. Talukdar, S. Buragohain, S. Kumar, V. Umakanth, N. Sarmah, and S. Mahapatra, "Effect of spectral response of solar cells on the module output when individual cells are shaded," *Solar Energy*, vol. 137, pp. 303–307, 2016, doi: 10.1016/j.solener.2016.08.032.

[25] T. N. Olayiwola, S. H. Hyun, and S. J. Choi, "Photovoltaic Modeling: A Comprehensive Analysis of the I–V Characteristic Curve," *Sustainability (Switzerland)*, vol. 16, no. 1, pp. 1–27, 2024, doi: 10.3390/su16010432.

[26] D. E. Parsons, G. Koutsourakis, and J. C. Blakesley, "Performance measurements for indoor photovoltaic devices: Classification of a novel light source," *APL Energy*, vol. 2, no. 1, pp. 1–9, 2024, doi: 10.1063/5.0186028.

[27] A. Soni, L. Pulikkool, R. Mulaveesala, S. K. Dubey, and D. S. Mehta, "Multi-Color Phosphor-Converted Wide Spectrum LED Light Source for Simultaneous Illumination and Visible Light Communication," *Photonics*, vol. 11, no. 10, Oct. 2024, doi: 10.3390/photonics11100914.

[28] T. Schneider, P. Dekker, R. Young, P. Blattner, and T. Poikonen, "EXTRAPOLATION OF PHOSPHOR CONVERTED WHITE LED SPECTRA BEYOND THE VISIBLE WAVELENGTH RANGE," International Commission on Illumination, Jun. 2019, pp. 1229–1237. doi: 10.25039/x46. 2019.po105.

[29] L. S. Shen, H. Y. Wu, L. J. Hsiao, C. H. Shih, and J. C. Hsu, "Led light improved by an optical filter to visible solar-like light with high color rendering," *Coatings*, vol. 11, no. 7, Jul. 2021, doi: 10.3390/coatings11070763.

[30] M. Spitschan, R. Lazar, and C. Cajochen, "Visual and non-visual properties of filters manipulating short-wavelength light," *Ophthalmic and Physiological Optics*, vol. 39, no. 6, pp. 459–468, Nov. 2019, doi: 10.1111/opo.12648.

[31] P. Kärhä *et al.*, "Measurement setup for differential spectral responsivity of solar cells," *Optical Review*, vol. 27, no. 2, pp. 195–204, 2020, doi: 10.1007/s10043-020-00584-x.